Brain Topogr (2017) 30:450–460
DOI 10.1007/s10548-016-0530-2

ORIGINAL PAPER

Effects of Stimulus Size and Contrast on the Initial Primary Visual Cortical Response in Humans

Nigel Gebodh[1] · M. Isabel Vanegas[1] · Simon P. Kelly[1,2]

Received: 28 June 2016 / Accepted: 11 October 2016 / Published online: 4 May 2017

Abstract Decades of intracranial electrophysiological investigation into the primary visual cortex (V1) have produced many fundamental insights into the computations carried out in low-level visual circuits of the brain. Some of the most important work has been simply concerned with the precise measurement of neural response variations as a function of elementary stimulus attributes such as contrast and size. Surprisingly, such simple but fundamental characterization of V1 responses has not been carried out in human electrophysiology. Here we report such a detailed characterization for the initial "C1" component of the scalp-recorded visual evoked potential (VEP). The C1 is known to be dominantly generated by initial afferent activation in V1, but is difficult to record reliably due to interindividual anatomical variability. We used pattern-pulse multifocal VEP mapping to identify a stimulus position that activates the left lower calcarine bank in each individual, and afterwards measured robust negative C1s over posterior midline scalp to gratings presented sequentially at that location. We found clear and systematic increases in C1 peak amplitude and decreases in peak latency with increasing size as well as with increasing contrast. With a sample of 15 subjects and ~180 trials per condition, reliable C1 amplitudes of −0.46 μV were evoked at as low a contrast as 3.13% and as large as −4.82 μV at 100% contrast, using stimuli of 3.33° diameter. A practical implication is that by placing sufficiently-sized stimuli to target favorable calcarine cortical loci, robust V1 responses can be measured at contrasts close to perceptual thresholds, which could greatly facilitate principled studies of early visual perception and attention.

Keywords C1 · Visual evoked potential · Primary visual cortex · Calcarine sulcus · Visual contrast · Stimulus size

Introduction

The primary visual cortex (area V1; Brodmann area 17) is one of the most extensively studied and well-characterized areas of the brain. A decades-long tradition of animal electrophysiological work in V1 forms the core of current knowledge on the fundamental mechanisms of mammalian vision (Hubel and Wiesel 1959; Wandell 1995). Over almost as long a period in human electrophysiology, the activity of area V1 has been examined through measurements of the initial electrical deflection or "component" in the scalp-recorded visual evoked potential (VEP) most widely known as the "C1." The C1's scalp distribution varies systematically with retinal location in a way that is exclusively consistent with the known geometry and retinotopic organization of V1 (Clark et al. 1995; Jeffreys and Axford 1972; Kelly et al. 2013b). Many insights into human vision have been gained through C1 measurements, especially regarding the modulation of early visual representations by bottom-up (Zhang et al. 2012) and top-down attention (Clark and Hillyard 1996; Itthipuripat et al. 2014; Kelly et al. 2008; Martínez et al. 1999) and attentional/perceptual "load" (Fu et al. 2009; Rauss et al. 2009), and regarding the neural changes that underpin perceptual learning (Bao et al. 2010; Pourtois et al. 2008; Wang et al. 2016; Zhang et al. 2015). Surprisingly, however, in stark

✉ Simon P. Kelly
spkell@gmail.com

[1] Department of Biomedical Engineering, The City College of the City University of New York, New York, NY, USA

[2] School of Electrical and Electronic Engineering, University College Dublin, Dublin 4, Belfield, Ireland

contrast against such extensive study of higher-order modulations, some of the most basic characteristics of the C1 response such as its dependence on the elementary stimulus attributes of contrast and size, have not been clearly established. The sensitivity of V1 neurons to such elementary factors has been central to understanding the computational roles of the area (Carandini et al. 2005), and therefore the lack of precise knowledge of homologous effects in humans represents a significant gap.

Effects of stimulus contrast and size have been extensively characterized at the single neuron level, particularly in cat and monkey. V1 spiking responses increase in magnitude as a monotonic function of contrast, characteristically saturating at higher contrasts (e.g. Albrecht and Hamilton 1982; Sclar et al. 1990). The relatively few studies that have scrutinized the initial onset of the neurons' transient response before reaching "steady-state" have additionally established that onset latency strongly and monotonically lengthens as a function of decreasing contrast (Albrecht et al. 2002; Gawne et al. 1996; Hu and Wang 2011). In fact, latency has been found to encode as much information about contrast as response magnitude and may well be central to how the brain discriminates contrast (Oram et al. 2002; Reich et al. 2001). As a function of size, V1 response magnitudes vary non-monotonically, increasing up to the point where an effective grating stimulus fills the classical receptive field of a given neuron, but then typically decreasing to a much lower asymptote as the size is further increased to cover the neuron's inhibitory surround (Cavanaugh et al. 2002; DeAngelis et al. 1994; Sceniak et al. 2001). This reflects the widely studied phenomenon of surround suppression, a salient example of redundancy-reducing normalization operations thought to pervade the visual system and beyond (Carandini and Heeger 2012).

An early line of research was dedicated to examining how the early visual evoked potential in humans changes as a function of pattern-onset stimulus parameters that have strong psychophysical effects (Jones and Keck 1978; Mihaylova et al. 1999; Parker et al. 1982; Vassilev et al. 1983). Although primarily focused on effects of spatial frequency, these studies also manipulated stimulus contrast and all reported reduced visual evoked response amplitudes and longer latencies for lower contrasts. However, despite using similar stimuli and recording protocols, the scalp potential deflection identified as the initial visual cortical response, on which these effects were measured, dramatically differed across studies. Comparing three prominent studies on the response to a grating of 4 cycles/degree (cpd) and 21–25% contrast, for example, Jones and Keck (1978) reported a negative peak deflection at approximately 85 ms, Parker et al. (1982) reported a positive peak at approximately 140 ms, and Vassilev et al. (1983) reported a negative peak at approximately 110 ms. This lack of consistency may be partly due to the small sample sizes used, and general tendency to focus on single-subject data. An additional critical factor, however, may be the use of very large (typically around 6 degrees, often full-screen) gratings positioned at fixation, with no accounting for the C1's sensitivity to spatial position or the potential for electric field cancellation due to opposed cortical surface orientations (Kelly et al. 2013b; Rauss et al. 2011). Psychophysical and event related potential (ERP) studies of cognitive processes such as attention and perceptual learning tend to employ peripheral, spatially constrained stimuli (usually within a single quadrant), which have recently been shown to evoke C1s with fundamentally different composition and waveshape (e.g. onset latency), as well as spatial frequency-dependence, than those evoked by foveal stimuli (Hansen et al. 2016). Thus, despite some earlier research having manipulated contrast, the contrast-dependency of the C1 component as typically defined and evoked in modern cognitive neuroscience is largely unknown. Reflecting this, recent studies examining the cellular contributions (Foxe et al. 2008) and attentional effects of the C1 (Itthipuripat et al. 2014; labelled as 'P1') at various levels of contrast have not taken latency changes into account in their measurements, opting instead to use fixed time windows across contrast levels.

Stimulus size dependencies of the initial visual response in humans are similarly unclear. Although effects of surround suppression due to static, pre-existing surround stimuli have been demonstrated in the steady-state (Vanegas et al. 2015) and transient VEPs (Ohtani et al. 2002) in humans, the expression of such suppressive interactions in the variations of V1 responses as a function of stimulus size, as meticulously examined in single-unit work, has not been examined in humans. The above issues, taken together, underline the need for a systematic examination of how C1 amplitude and latency varies as a function of contrast and size for peripheral stimuli. The present study undertook such a characterization, with the dual purpose of bridging to fundamental animal electrophysiology work, and providing a useful guide to effective stimulus design for perceptual/cognitive paradigms relying on the C1 component.

Due to the wide variation in human visual cortical anatomy across individuals (Amunts et al. 2000; Rademacher et al. 1993), the C1 component is known to be difficult to measure reliably (Kelly et al. 2008; Rauss et al. 2011). Increasingly, this reliability issue has been addressed by tailoring stimulus locations to individuals, typically on the basis of preliminary spatial field mapping (Bao et al. 2010; Kelly et al. 2008; Zhang et al. 2015). In the current study we employed an individualized mapping procedure using pattern-pulse multifocal (PPM) VEPs based on m-sequences (James 2003), which allow measurement

of neural responses to a large number of spatial locations stimulated simultaneously. This preliminary mapping session enabled us to map out changes in C1 scalp distribution as a function of stimulus location (polar angle) and thereby to select a stimulus location evoking a robust, approximately midline-focused, negative C1 in each subject before asking them to view stimuli of different sizes and contrasts at that same retinal location in the main experiment.

Materials and Methods

Apparatus

All visual stimulation was carried out in a closed and fully dark, sound-attenuated and electromagnetically isolated room, with the subject comfortably seated with their head resting in a chin-rest. Stimuli were presented on a gamma-corrected CRT monitor (Dell M782), placed 57 cm directly in front of the eyes of the subject. The background brightness of the screen was set to give a luminance of 65.2 cd/m^2, the midpoint between the minimum (black, brightness level 0, 0.2 cd/m^2) and maximum (white, level 255, 130.2 cd/m^2) luminance of the monitor. Eye position was continuously recorded throughout the visual stimulation at a sample rate of 1000 Hz using an Eyelink 1000 eye tracker (SR Research).

Subjects

Sixteen human observers with normal or corrected-to-normal vision participated in the main experiment measuring effects of size and contrast on the C1 component of the transient VEP. Twelve of these subjects were recruited on the basis of multifocal mapping data already acquired for a separate study; specifically, the existing mapping data of 21 subjects were consulted and 17 met our inclusion criteria (see "Individualized Mapping" section), and of those, 12 were available and willing to return to participate in the current experiment. Four additional participants were then recruited, each of whom met the inclusion criteria. The size-contrast data of one subject of the 16 were excluded because less than half of their trials remained after artifact rejection, leaving a final group of 15 (6 female, 9 male), all between the ages of 19–33 years (mean = 25.6 ± 4.53 years). All procedures were conducted in accordance with the ethical guidelines set forth by the Declaration of Helsinki in 1964 and its later amendments; and were approved by the Institutional Review Board of The City College of New York. Written informed consent was obtained from all subjects. Subjects were compensated at a rate of $12/h for their time.

Individualized Mapping

In the individualized mapping procedure, subjects passively viewed a pattern-pulse multifocal stimulus consisting of 32 equal-sized radial segments of an annular checkerboard pattern, each driven by an independent m-sequence and thus allowing derivation of neural responses to each segment individually despite simultaneous presentation (James 2003; see also Vanegas et al. 2013). An m-sequence or maximum-length sequence is a pseudo randomized, binary, linearly shifted sequence generated by primitive polynomials (Baseler et al. 1994), which allows efficient estimation of event-related responses (Buracas and Boynton 2002). The annular stimulus area extended from 3 to 6 degrees of eccentricity (Fig. 1a) and each segment consisted of 2 × 4 checks extending over 11.25° of polar angle. For this procedure the monitor was set to 800 × 600 pixel resolution and 100-Hz refresh rate, providing 10-ms temporal resolution for visual pulse trains. The primary m-sequence was generated afresh for each trial, by first generating a standard 4095-point m-sequence which randomly flips between values −1 and 1 (function 'mseq'; Buracas and Boynton 2002), converting to pulses by setting to zero every point except those transitioning from −1 to 1, thinning out by keeping only every 4th pulse, and finally extending the duration of every pulse to two screen frames (20 ms). This results in a 41-s pulse train with on average 6.25 pulses per second. The pulse train driving each of the other 31 segments was formed by shifting the original sequence in steps of 50 frames (500 ms). Ten trials of such stimulation were presented within a single block for each subject.

Pattern-pulse VEPs were derived for each of the 32 segments using multiple linear regression (James 2003), and topographies integrated over 10-ms time ranges were plotted between 50 and 90 ms in order to identify, by eye, a segment from which a strong, approximately midline-focused, negative C1 deflection was evoked (Fig. 1). For the sake of homogeneity we opted to select a location in the right visual field only, typically slightly above the horizontal meridian, where a midline negative focus is generated from the left lower bank of the calcarine sulcus according to the cruciform model (Clark et al. 1995; Kelly et al. 2013b; Wandell et al. 2009). Subjects for whom a clear right-hemifield-evoked C1 component as described above could not be identified were not asked to participate in the main experiment with size and contrast manipulations. Four subjects of the total 25 mapping datasets consulted were excluded in this way, for the reason that any negative potential observed before the 90-ms timepoint was either extremely weak, unfocused topographically or extremely anterior or posterior to the typical parietal/occipital midline region.

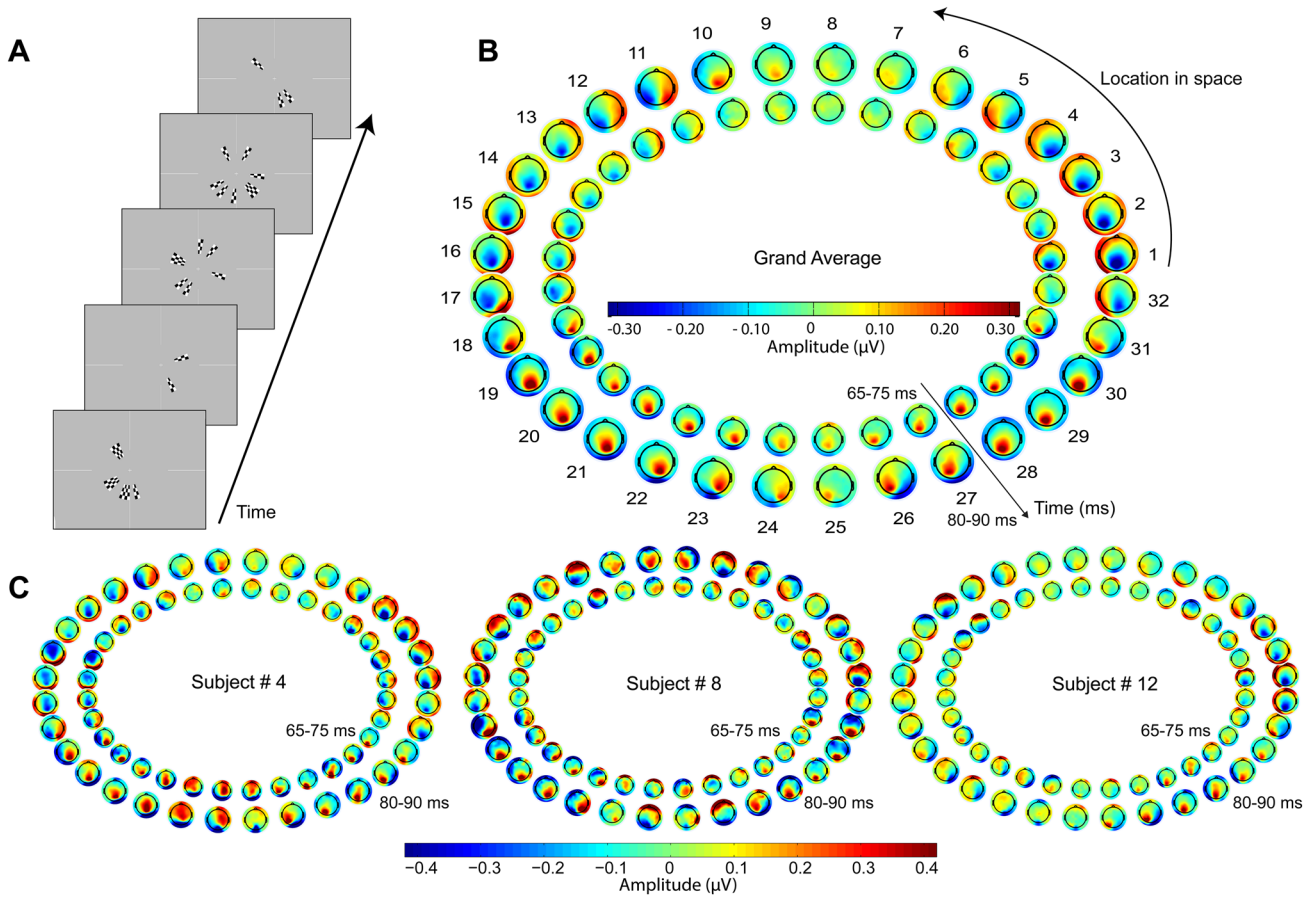

Fig. 1 Data from preliminary individualized mapping procedure. **a** Shown are randomly chosen screen captures during the pattern-pulse multifocal stimulation. **b** The grand average scalp potential topographies across all 15 subjects of the earliest component of the pattern-pulse VEP for each of the 32 stimulus locations, in the time frames of 65–75 ms (*inner*) and 80–90 ms (*outer*). The typical average topographic shifts consistent with calcarine cortical physiology (see Kelly et al. 2013b) are readily observable, with remarkable symmetry about the vertical meridian. Segments 18 and 31, for example, correspond to the fundus of the calcarine sulcus in the right hemisphere for lower left visual field stimulation (18) and in the left hemisphere for lower right visual field stimulation (31), respectively (Clark et al. 1995). **c** Topographies of three individual subjects selected to highlight the inter-subject variability in topographic dependence on location, consistent with the well-known variability in calcarine cortical size and geometry (Amunts et al. 2000; Rademacher et al. 1993). Whereas Subject 4 (*left*) exhibited typical dipolar field shifts as a function of polar angle with vertical symmetry, Subjects 8 and 12 exhibited maps that clearly diverged from the average pattern in terms of points of apparent dipole rotation and asymmetry. For each individual, a single right-hemifield polar angle was identified at which a strong, approximately midline-focused, negative C1 was evoked, which was then used in the main experiment manipulating stimulus contrast and size. Polar angle of the thus chosen segments ranged from −11.25° to 45° (mean 18.00°; SD ±14.13°) relative to the right horizontal meridian

Main Experimental Task

Having identified a suitable stimulus location from a given subject's multifocal mapping data, the main experimental task was run, in which a series of grating stimuli varying in size and contrast were presented at this individually-optimized location. This main task was run in the same recording session in some subjects, but after several months delay in some (range 0–500 days, median 46 days). The grating stimuli consisted of "center-saturated" Gabor patches, which were created by taking a standard Gabor stimulus and clipping its luminance deviation profile (difference with respect to mean/background luminance level) at half the maximum deviation, and then scaling the whole pattern to provide the appropriate contrast values at the center. This results in a central radius of 1.18 times the Gaussian sigma value in which contrast is constant, and a gradual fading of contrast beyond that radius, thus providing a stimulus akin to a circular grating as typically used in single-unit studies manipulating stimulus size (e.g. Cavanaugh et al. 2002), but with fading rather than discrete edges (see Fig. 2). We avoided discrete edges to minimize stimulus energy at orientations other than the central orientation. We varied the contrast of the central grating area across six levels (3.13, 6.25, 12.5, 25, 50, and 100%), and tested four sizes (diameters of the central constant-contrast area of 0.83°, 1.67°,

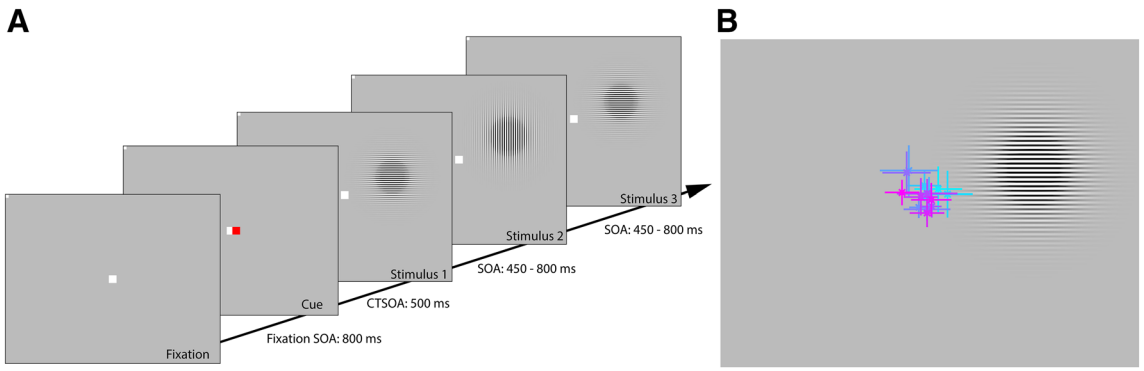

Fig. 2 Size-contrast stimulation paradigm. **a** Each trial consisted of a warning cue followed by 48 stimuli of varying contrast, size, and orientation, presented one after another. After each trial, subjects reported whether there was a greater number of horizontal versus vertical gratings. Each block contained 10 trials of 48 stimuli and all subjects underwent between 10 and 12 blocks, resulting in an overall testing time of approximately 90–120 min on average. Note that fixation and cue size are exaggerated for the purposes of clarity, and were much smaller in practice. **b** Mean eye position during the extracted EEG epochs with 95% confidence intervals for each individual subject (shown in *different colors*) superimposed on a screen capture of the task display. Screen capture is to scale but cropped in order to highlight individuals' eye positions. (Color figure online)

2.5° and 3.33°, respectively) and two orientations (90° and 180°), together creating a total of 48 unique stimulus conditions. The gratings had a spatial frequency of 5 cycles/degree for all conditions since this was within the range of spatial frequencies shown to evoke robust C1 components (Rebai et al. 1998). It should be noted however, that the C1 has been found to be very sensitive to spatial frequency and thus caution should be taken in generalizing our precise measurements to other spatial frequencies. All stimuli were presented on the uniform gray background at a single location with an eccentricity of 5 degrees and polar angle selected from multifocal mapping where the response was maximal in a given subject, with a duration of 100 ms. The monitor was set to 60 Hz refresh rate and 1280×960 pixel resolution in this case, to maximize spatial resolution on the monitor for precise size manipulation. It should be noted that no effort was made to exactly match the spatial frequency content of the multifocal mapping stimulus and the discrete stimuli presented in the main experiment. We have implicitly assumed that, although strength and timing of temporal waveforms might change, the manner in which the initial VEP topography varies as a function of polar angle in the visual field does not change appreciably with spatial frequency.

In the task, subjects viewed a sequence of 48 grating stimuli in each trial, and, after the final one, indicated their best guess as to whether the majority of gratings were vertically versus horizontally oriented. This discrimination task, on a stimulus dimension (orientation) orthogonal to the parameters of interest (size and contrast), was designed simply to hold the subjects' attention for the duration of visual stimulation. Ten trials were run in each block, and the total 480 stimuli in a block included exactly ten of each stimulus condition (contrast × size × orientation), which were randomly ordered and distributed among the ten trials. Trial timing was as follows: a central fixation spot (6×6 pixels) first appeared, followed 800 ms later by a 500-ms warning cue consisting of a red spot of the same size presented 4 pixels to the right of center, after which the 48 gratings for that trial were presented with pseudorandomized stimulus onset asynchronies (SOAs) ranging from 450 to 800 ms inclusive, in steps of 50 ms. Subjects were asked to maintain fixation on the central spot throughout stimulation (see Fig. 2b). At the end of each trial of 48 stimuli, subjects indicated whether they saw a greater number of vertical versus horizontal grating stimuli by clicking a left versus right mouse button, respectively. Immediate feedback on whether their choice was correct or incorrect was given after their selection was made. The subject initiated the next trial by clicking either mouse buttons. A percentage accuracy score was presented at the end of each block of ten trials. Each subject underwent between 10 and 12 blocks of trials, each of which lasted approximately 5–8 min, resulting in an overall testing time of approximately 90–120 min on average. This provided a minimum of 100 trials for each unique stimulus condition.

EEG Recording and Analysis

Continuous EEG data were acquired from a 97-channel electrode montage (Brain Products DC amps and actiCAP) with an online 60-Hz notch filter and sample rate of 500 Hz. Data were online referenced to standard site FCz and electrode impedances maintained stable below 50 kΩ. For multifocal pattern-pulse VEP analysis, there was an additional online high-pass filter with 0.5 Hz

cut-off, and offline, data were further filtered in the range 1–45 Hz (4th-order Butterworth bandpass with these cut-offs) and re-referenced to the average of all channels, in accordance with the original study of the pattern-pulse multifocal VEP method (James 2003). For analysis of transient VEPs in the main experiment, the data were recorded in DC mode and were low-pass filtered offline by convolution (i.e. finite impulse response, linear-phase) with a 58-tap hanning-windowed sinc function which provided a 3-dB corner frequency of 41.5 Hz and a local extremum of attenuation coinciding with the mains frequency (60 Hz), while also avoiding ringing artifacts (Widmann and Schroger 2012). Channels identified as excessively noisy or saturating during online recording were noted and interpolated (spherical splines) in offline analysis. Data were then re-referenced to the mean of the mastoid channels, in order to maximize VEP amplitude for cortical sources located on the banks of the calcarine sulcus (Clark et al. 1995). Note that the filter settings and offline referencing were different in the mapping and main experimental sessions because they were tailored to the distinct purposes of each; in the current study we do not draw direct comparisons between multifocal and transient VEPs but rather employ the former to optimize stimulus locations for the latter. Stimulus-locked epochs extending from −100 to 400 ms relative to onset were extracted, baseline-corrected relative to the interval −30 to 30 ms, and subjected to an artifact rejection criterion of 50 μV to remove trials with eye movements, muscle activity, and/or blinks. A cluster of four neighboring electrodes lying at the negative topographic focus was identified for each individual from data collapsed across all stimulus conditions. The individual average C1 waveform for each of the 24 relevant stimulus conditions (6 contrasts × 4 sizes, with orientation collapsed) was then computed as the average across these four electrodes. Since subjects were performing a sustained discrimination task, anticipatory negative-going slow potentials were observed in the baseline. To remove this influence on measurements of the bottom-up evoked C1 component, we performed a linear drift correction by computing a least-squares linear fit over the interval −80 to 20 ms relative to stimulus onset in the individual average waveform collapsed across all conditions, extending that line through the entire epoch and then subtracting it out from each individual condition (Fig. 3). We chose a baseline interval extending slightly into the post-stimulus period so that the slope of the anticipatory shift is measured close in time to the evoked potential onset, but certainly without overlapping it. The slopes thus measured ranged from −0.0064 to 0.0024 μV/ms and had a median value of −0.0021 μV/ms. All offline analysis was performed using in-house scripts written in Matlab (R2013b; MathWorks, Natick, MA) with raw data-reading, channel interpolation and topographic plot functions from the EEGLAB toolbox (Delorme and Makeig 2004).

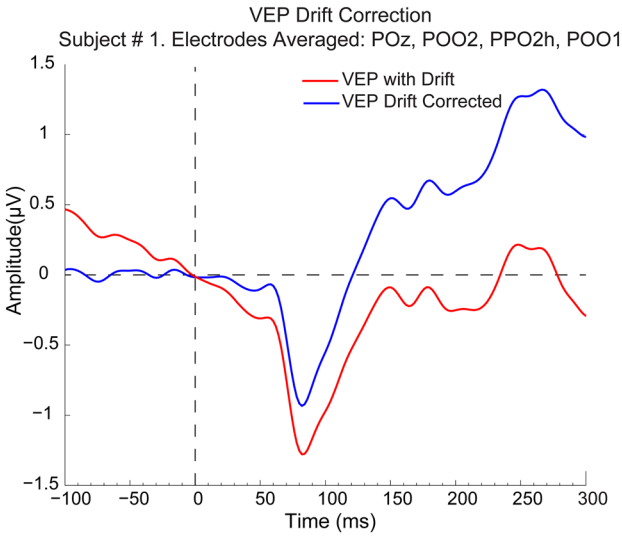

Fig. 3 VEP waveform drift correction. The trial-averaged VEP waveform for each stimulus condition and each subject, averaged across a cluster of four electrodes at the C1's negative focus, were drift-corrected by computing a linear least squares fit from −80 to 20 ms relative to stimulus onset, extending that line through the entire epoch, and then subtracting that line from the waveform. As the example of Subject 1 shows, this successfully flattens the baseline and guards against over-estimation of negative C1 amplitude due to anticipatory potential shifts

Our main analysis goal was to quantify as precisely as possible the variation in C1 peak amplitude and latency as a function of both size and contrast. In order to facilitate reliable identification of C1 peaks at even the lower contrasts and sizes, we applied a peak-finding algorithm to the grand-average waveforms, for each unique contrast and size condition. For each size, the peak latency was first detected for the 100% contrast condition by simply finding the global minimum point in a 0–150 ms time window. Then for the 50% contrast condition of the same size, the closest local minimum in time with respect to the 100% contrast peak latency was computed. This local minimum search was conducted in both the forward and backward directions in an unbiased way. Next the peak latency for the 25% contrast was computed as the closest local minimum to the 50% peak latency, and so on down to 3.13% contrast. In order to compute the standard error of the peak amplitude and latency estimates across subjects, we carried out a Jackknifing routine, whereby the above peak-finding algorithm was applied repeatedly to grand-average data with each subject left out at a time. This procedure has been found to produce more reliable latency estimates than the approach of quantifying latency at the individual subject level, which is especially vulnerable to misestimation due

to typical levels of noise within single-subject data (Miller et al. 2009). For consistency with the latency plot, we plot the mean and standard error at each contrast and size for amplitude values produced by the same jackknifing procedure. As a check, we also quantified mean and standard error for amplitude in the more standard way by conducting the peak-finding algorithm on the grand average of all 15 subjects but then taking individual amplitude measurements at the determined contrast/size-dependent latencies (rather than resampling). The plots were almost identical: the largest divergence from the resampling-based values shown in Fig. 4b in the mean values among any contrast or size was 2%, while the largest divergence in standard error was 3%.

We quantified and plotted C1 peak amplitude and latency only for size/contrast conditions that evoked a reliable C1 component. To determine reliability, we repeated the above estimation of average peak amplitude and latency for a "null" dataset constructed by extracting 250-ms epochs from the baseline periods of all trials (i.e., ending at stimulus onset time) in which no C1 is present, randomly assigning conditions to trials with the number of trials per condition matched to the real data, averaging in the usual way for each condition and drift-correcting in the same way as the real data. In the peak search for each contrast, the latency of the next highest contrast was taken from the real data estimates rather than the null data from the same permutation, to ensure that baseline correction timing was

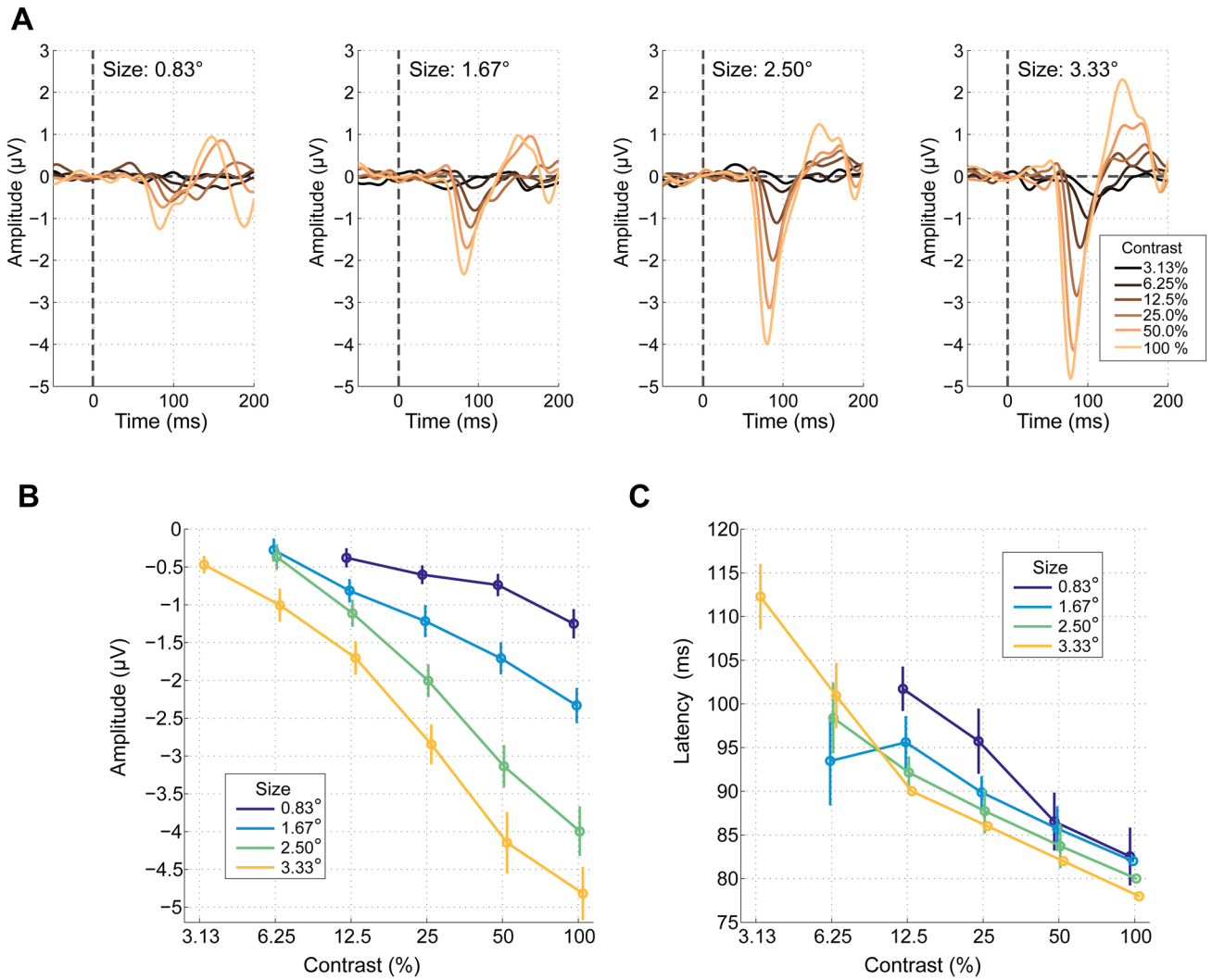

Fig. 4 C1 component variation as a function of size and contrast. **a** Visual evoked potential waveforms for each size and contrast. Amplitude clearly increased with both contrast and size. **b** The contrast response function of C1 peak amplitude exhibited a monotonic increase in negative potential with increasing stimulus diameter and contrast. Conditions for which a reliable C1 component was not elicited are omitted. *Error bars* reflect the standard error of the mean across subjects, estimated through a Jackknife procedure. **c** C1 peak latency increased strongly with decreasing contrast, and stimulus size

matched across real and null peak searches. Repeating this 500 times with a different random condition-permutation each time provided a null distribution of C1 peak amplitudes for each condition, which can arise by chance in trial-averaged EEG signals that in fact have no evoked C1 component. The real C1 in a given condition was labelled as reliable if its amplitude was more negative than 95% of amplitudes in the null distribution for that same condition.

To assess whether the C1 amplitude variations with stimulus size are consistent with suppressive interactions of the kind characterized in animals (Cavanaugh et al. 2002; DeAngelis et al. 1994), or alternatively, could be accounted for simply by a summation of non-interacting neural responses, we fit functions of the form $y = Ax^B$ to the measures of amplitude (y) varying as a function of size (x) at each contrast for each subject, and tested whether the median value of exponent parameter B was significantly smaller than 2. This is based on the logic that the global sum of non-interacting neural responses would scale linearly with stimulus area, and hence as a quadratic function (i.e., $B = 2$) of size defined in terms of diameter (recall area of a circle $= \pi \times \text{radius}^2$). Parameters A and B were fit by exhaustive search, specifically, by quantifying the sum of squared errors (SSE) between the real and predicted amplitude values for each of a large set of values of A (ranging from 0 to 2) and B (ranging from 0 to 4), and finding the (A, B) pair producing the smallest SSE value. No additive offset term was included based on the assumption that for zero size (i.e., no stimulus), no evoked potential deflection can occur relative to baseline. Individual subject C1 amplitude for this test was measured as the mean amplitude across a fixed 20-ms interval centered on the average peak latency for each contrast × size condition.

Results

Figure 4a shows the grand-average evoked potential waveforms for each grating size and contrast, with orientation collapsed. C1 peak amplitudes were in general remarkably large for such spatially-constricted stimuli, reaching almost 5 μV for the highest contrast and largest size. In comparison, amplitudes have not tended to exceed 2 μV for similar stimuli in previous work (Bao et al. 2010; Clark et al. 1995; Clark and Hillyard 1996; Di Russo et al. 2002; Martínez et al. 1999). This attests the effectiveness of the mapping procedure for individualized stimulus placement. C1 peak amplitude increased systematically as a function of both size and contrast.

Reliable C1s were found for all contrasts at the largest stimulus size (3.33° diameter), including the lowest contrast of 3.13% (Fig. 4b). For smaller sizes, higher contrasts were needed to evoke reliable C1 components at the grand-average level (6.25% contrast for sizes 1.67° and 2.5° and 12.5% for 0.83°).

C1 peak latencies also exhibited strong variation with contrast, increasing from 78 ms at 100% to 112 ms at 3.13% contrast for the largest stimulus size (Fig. 4c). More unexpectedly, there was an apparent shortening of peak latency with stimulus size for most contrast levels. To statistically test for the reliability of this effect, we performed a permutation test at each contrast level at which there was more than one reliable C1 (thus excluding 3.13%). We first quantified the real effect of size as the slope of a linear regression of peak latency onto size in the grand average at a given contrast, and then computed this same slope measure for 1000 shuffled versions of the dataset where sizes within that same contrast level were randomly permuted, thus allowing comparison (i.e., percentile calculation) of the real slope value to the null distribution where no size effect exists. This revealed a significant decrease in peak latency with size at contrast levels 100, 50, 25 and 12.5% (all $p < 0.01$) but no significant effect at 6.25%.

Figure 5 shows the average C1 amplitudes as a function of stimulus diameter (filled circles), fit by the function $y = Ax^B$ (solid), along with, for comparison, the function fit with the constraint $B = 2$ (i.e., linear increase in amplitude with stimulus area; dashed). The median value of exponent B for the contrasts at which all four sizes evoked a reliable C1 (12.5, 25, 50, 100%) was (1.18, 1.24, 1.25, 0.94), all four of which were significantly different from 2 (sign test; all $p < 0.001$). This indicates the operation of significant

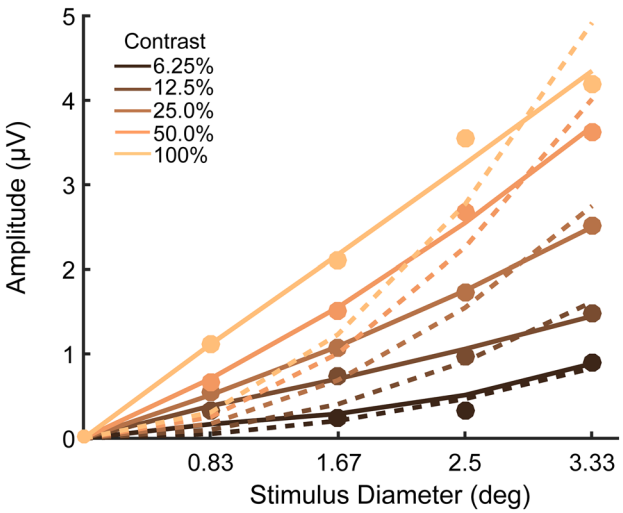

Fig. 5 C1 component amplitude varied sub-quadratically as a function of stimulus diameter. *Filled circles* mark real data points reflecting average C1 amplitude in 20-ms time windows centered on grand-average peak latency. *Solid lines* show the best fitting function of the form $y = Ax^B$ with both A and B free to vary. *Dashed lines* show the best fits of the function with B constrained to be equal to 2, as would be the case if C1 amplitude increased linearly with stimulus area

suppressive interactions at the neuronal level, whereby the tendency for neuronal responses to be relatively suppressed with stimulus areas extending beyond their excitatory receptive fields counteracts the tendency for increased stimulus area to excite a greater number of neurons that contribute to the globally measured response.

Discussion

In the present study we made precise measurements of C1 component amplitude and latency as a function of the elementary stimulus attributes of contrast and size. Using a preliminary pattern-pulse-based mapping procedure, we were able to measure reliable C1 components for contrast levels as low as 3.13% for the largest stimulus size tested, with amplitudes reaching as high as almost 5 μV for the highest contrast and largest size. These results are based on a sample of fifteen subjects and mean ± SD trial count of 178 ± 26 per condition, which are very typical of visual evoked potential studies. This highlights the potential for such a mapping procedure, which takes less than 10 min to record and analyze, to facilitate experimental investigation of cortical responses underlying psychophysical detection and discrimination at near-threshold contrasts, and by extension the effects of cognitive processes such as attention and perceptual learning on such psychophysically-relevant neural responses.

Interestingly, contrast response functions showed less tendency to saturate than their single-neuron counterparts typically show (Albrecht and Hamilton 1982), which could be a result of global summation over neurons with widely varying saturating contrast, and/or the fact that we are measuring only the very initial portion of the response, during which studies in cat V1 have also demonstrated initially non-saturating contrast-response profiles (Albrecht et al. 2002; Hu and Wang 2011). More generally, it is important to note that although a major aim of the current study was to follow the lead of seminal animal intracranial electrophysiology work characterizing sensitivity to contrast and size, parallels drawn between species need to be tempered by due consideration of the differences in the nature of the measurements: most saliently, here we have quantified mean and variability in amplitude and latency across human subjects, not neurons, and it is not possible to infer the latter from the former.

Consistent with the original study of Jeffreys and Axford (1972) and more recent studies following up on the same theme (Clark et al. 1995; Kelly et al. 2013b), we observed systematic shifts in the average scalp distribution of the C1 component as a function of polar angle in the visual field that are highly consistent with the "cruciform model" describing retinotopic organisation and dipolar field orientation over the outer and inner banks of the calcarine sulcus (Fig. 1b). Studies based on scalp current density analysis (Foxe and Simpson 2002) and retinotopically constrained source modeling (Ales et al. 2010; Hagler 2014; Hagler et al. 2009) have provided evidence supporting the assumption that the C1 component is unlikely to reflect purely V1 activity for its entire duration, and may have mixed contributions from neighboring extrastriate areas such as V2 and V3 by the time it peaks. However, recent forward modeling of average scalp distributions generated purely from V2 and V3 revealed that these areas, when stimulated from visual field locations targeting the horizontally-oriented calcarine banks in V1, have scalp projections that significantly overlap those for area V1 but with reversed polarity (Ales et al. 2010, 2013; see also and Kelly et al. 2013a for context). This indicates that any contribution from V2/V3 during the C1 would tend to reduce its amplitude and counter the V1 contribution, rather than masquerade as a V1 contribution (Kelly et al. 2013b). In light of this, it is possible that the systematic variation of peak latency as a function of contrast and, to a lesser extent, size, may be partly driven by onset latency variations in areas V2/V3, because the C1 peak may mark the point where the rate of V2/V3 activation begins to exceed the rate of V1 activation rather than the peak of V1 activation on its own. To the extent that this is the case, our peak latency values would be underestimated with respect to the real peak latency in area V1 alone. Using retinotopy constrained source estimation, Hagler (2014) reported a lengthening in V1 peak latency from 78 ms at close to 100% contrast to 100 ms at 15%, a relative delay that is slightly longer than we observed for most of our stimulus sizes. At the same time, the amount by which peak latency is delayed with decreasing contrast in our data—for example the relative delay of approximately 10 ms for 25% compared to 100% contrast gratings—is similar to that observed in the peak firing rate latencies of cats (Hu and Wang 2011) and in the V1 onset latencies measured using voltage sensitive dye imaging in monkeys (Sit et al. 2009). Given the uncertainty regarding overlapping V2/V3 contributions, however, our peak latency estimates should be taken to apply to the scalp-recorded C1 component rather than the underlying neural source in V1 that dominantly generates it.

As in previous studies (e.g. Kelly et al. 2008), the maps of C1 topography as a function of polar angle varied significantly across individual subjects. However, for the vast majority of subjects, the same topographic shifts expected from the cruciform model could be identified as one proceeds through the locations, but with these expected shifts happening at variable points along the way, and exhibiting slight offsets on the scalp from one subject to another (Fig. 1c). This variability in the

multifocal maps are most likely due to anatomical variations in calcarine morphology (Amunts et al. 2000; Rademacher et al. 1993; Stensaas et al. 1974) and stresses the importance of individualized stimulus positioning in order to generate reliable VEPs from V1.

Variations in early VEP component latency and amplitude as a function of contrast have been previously reported (Jones and Keck 1978; Mihaylova et al. 1999; Parker et al. 1982; Vassilev et al. 2002) but those studies presented only very large gratings at fixation and varied widely in terms of the timing and polarity of the potential deflection regarded as the initial response peak. The present measurements are relevant for the kinds of stimuli used commonly in recent work on visual perception and cognition. It is important to note that those early studies additionally reported dramatic variations in VEP component latency and amplitude as a function of spatial frequency of the gratings used, and therefore the variations we report here are unlikely to take the same absolute values if spatial frequencies other than 5 cpd are used, especially given the known differences in spatial frequency sensitivity for different cell types (e.g. magnocellular and parvocellular) which also differ in their temporal properties. It could be plausibly assumed, however, that the pattern of scaling with contrast and size would be qualitatively conserved.

Acknowledgements The authors are grateful to Azeezat Azeez and Annabelle Blangero for helpful discussions at the outset of the project. This research was supported by the National Institute of General Medical Sciences of the National Institutes of Health under Award Number SC2GM099626.

Compliance with Ethical Standards

Conflict of interest The authors declare no competing financial interests.

References

Albrecht DG, Hamilton DB (1982) Striate cortex of monkey and cat: contrast response function. J Neurophysiol 48:217–237

Albrecht DG, Geisler WS, Frazor RA, Crane AM (2002) Visual cortex neurons of monkeys and cats: temporal dynamics of the contrast response function. J Neurophysiol 88:888–913

Ales JM, Yates JL, Norcia AM (2010) V1 is not uniquely identified by polarity reversals of responses to upper and lower visual field stimuli. Neuroimage 52:1401–1409. doi:10.1016/j.neuroimage.2010.05.016

Ales JM, Yates JL, Norcia AM (2013) On determining the intracranial sources of visual evoked potentials from scalp topography: a reply to Kelly et al. (this issue). Neuroimage 64:703–711. doi:10.1016/j.neuroimage.2012.09.009

Amunts K, Malikovic A, Mohlberg H, Schormann T, Zilles K (2000) Brodmann's areas 17 and 18 brought into stereotaxic space—where and how variable? Neuroimage 11:66–84

Bao M, Yang L, Rios C, He B, Engel SA (2010) Perceptual learning increases the strength of the earliest signals in visual cortex. J Neurosci 30:15080–15084

Baseler H, Sutter E, Klein S, Carney T (1994) The topography of visual evoked response properties across the visual field. Electroencephalogr Clin Neurophysiol 90:65–81

Buracas GT, Boynton GM (2002) Efficient design of event-related fMRI experiments using M-sequences. Neuroimage 16:801–813

Carandini M, Heeger DJ (2012) Normalization as a canonical neural computation. Nat Rev Neurosci 13:51–62. doi:10.1038/nrn3136

Carandini M et al (2005) Do we know what the early visual system does? J Neurosci 25:10577–10597. doi:10.1523/JNEUROSCI.3726-05.2005

Cavanaugh JR, Bair W, Movshon JA (2002) Nature and interaction of signals from the receptive field center and surround in macaque V1 neurons. J Neurophysiol 88:2530–2546. doi:10.1152/jn.00692.2001

Clark VP, Hillyard SA (1996) Spatial selective attention affects early extrastriate but not striate components of the visual evoked potential. J Cogn Neurosci 8:387–402

Clark VP, Fan S, Hillyard SA (1995) Identification of early visual evoked potential generators by retinotopic and topographic analyses. Hum Brain Mapp 2:170–187

DeAngelis GC, Freeman RD, Ohzawa I (1994) Length and width tuning of neurons in the cat's primary visual cortex. J Neurophysiol 71:347–374

Delorme A, Makeig S (2004) EEGLAB: an open source toolbox for analysis of single-trial EEG dynamics including independent component analysis. J Neurosci Methods 134:9–21. doi:10.1016/j.jneumeth.2003.10.009

Di Russo F, Martinez A, Sereno MI, Pitzalis S, Hillyard SA (2002) Cortical sources of the early components of the visual evoked potential. Hum Brain Mapp 15:95–111

Foxe JJ, Simpson GV (2002) Flow of activation from V1 to frontal cortex in humans. A framework for defining "early" visual processing. Exp Brain Res 142:139–150. doi:10.1007/s00221-001-0906-7

Foxe JJ, Strugstad EC, Sehatpour P, Molholm S, Pasieka W, Schroeder CE, McCourt ME (2008) Parvocellular and magnocellular contributions to the initial generators of the visual evoked potential: high-density electrical mapping of the "C1" component. Brain Topogr 21:11–21

Fu S, Huang Y, Luo Y, Wang Y, Fedota J, Greenwood PM, Parasuraman R (2009) Perceptual load interacts with involuntary attention at early processing stages: event-related potential studies. Neuroimage 48:191–199

Gawne TJ, Kjaer TW, Richmond BJ (1996) Latency: another potential code for feature binding in striate cortex. J Neurophysiol 76:1356–1360

Hagler DJ Jr, Halgren E, Martinez A, Huang M, Hillyard SA, Dale AM (2009) Source estimates for MEG/EEG visual evoked responses constrained by multiple, retinotopically-mapped stimulus locations. Hum Brain Mapp 30:1290–1309. doi:10.1002/hbm.20597

Hagler DJ Jr (2014) Optimization of retinotopy constrained source estimation constrained by prior. Hum Brain Mapp 35:1815–1833. doi:10.1002/hbm.22293

Hansen BC, Haun AM, Johnson AP, Ellemberg D (2016) On the Differentiation of foveal and peripheral early visual evoked potentials. Brain Topogr 29:506–514. doi:10.1007/s10548-016-0475-5

Hu M, Wang Y (2011) Rapid dynamics of contrast responses in the cat primary visual cortex. PLoS ONE 6:e25410. doi:10.1371/journal.pone.0025410

Hubel DH, Wiesel TN (1959) Receptive fields of single neurones in the cat's striate cortex. J Physiol 148:574–591

Itthipuripat S, Ester EF, Deering S, Serences JT (2014) Sensory gain outperforms efficient readout mechanisms in predicting attention-related improvements in behavior. J Neurosci 34:13384–13398

James AC (2003) The pattern-pulse multifocal visual evoked potential. Invest Ophthalmol Vis Sci 44:879–890

Jeffreys DA, Axford JG (1972) Source locations of pattern-specific components of human visual evoked potentials. I. Component of striate cortical origin. Exp Brain Res 16:1–21

Jones R, Keck MJ (1978) Visual evoked response as a function of grating spatial frequency. Invest Ophthalmol Vis Sci 17:652–659

Kelly SP, Gomez-Ramirez M, Foxe JJ (2008) Spatial attention modulates initial afferent activity in human primary visual cortex. Cereb Cortex 18:2629–2636. doi:10.1093/cercor/bhn022

Kelly SP, Schroeder CE, Lalor EC (2013a) What does polarity inversion of extrastriate activity tell us about striate contributions to the early VEP? A comment on Ales et al. (2010). Neuroimage 76:442–445. doi:10.1016/j.neuroimage.2012.03.081

Kelly SP, Vanegas IM, Schroeder CE, Lalor EC (2013b) The cruciform model of striate generation of the early VEP re-illustrated not revoked: a reply to Ales et al. (2013). Neuroimage 82:154–159

Martínez A et al (1999) Involvement of striate and extrastriate visual cortical areas in spatial attention. Nat Neurosci 2:364–369. doi:10.1038/7274

Mihaylova M, Stomonyakov V, Vassilev A (1999) Peripheral and central delay in processing high spatial frequencies: reaction time and VEP latency studies. Vision Res 39:699–705

Miller J, Ulrich R, Schwarz W (2009) Why jackknifing yields good latency estimates. Psychophysiology 46:300–312. doi:10.1111/j.1469-8986.2008.00761.x

Ohtani Y, Okamura S, Yoshida Y, Toyama K, Ejima Y (2002) Surround suppression in the human visual cortex: an analysis using magnetoencephalography. Vision Res 42:1825–1835

Oram MW, Xiao D, Dritschel B, Payne KR (2002) The temporal resolution of neural codes: does response latency have a unique role? Philos Trans R Soc Lond B 357:987–1001. doi:10.1098/rstb.2002.1113

Parker DM, Salzen EA, Lishman JR (1982) Visual-evoked responses elicited by the onset and offset of sinusoidal gratings: latency, waveform, and topographic characteristics. Invest Ophthalmol Vis Sci 22:675–680

Pourtois G, Rauss KS, Vuilleumier P, Schwartz S (2008) Effects of perceptual learning on primary visual cortex activity in humans. Vision Res 48:55–62

Rademacher J, Caviness VS Jr, Steinmetz H, Galaburda AM (1993) Topographical variation of the human primary cortices: implications for neuroimaging, brain mapping, and neurobiology. Cereb Cortex 3:313–329

Rauss KS, Pourtois G, Vuilleumier P, Schwartz S (2009) Attentional load modifies early activity in human primary visual cortex. Hum Brain Mapp 30:1723–1733. doi:10.1002/hbm.20636

Rauss K, Schwartz S, Pourtois G (2011) Top-down effects on early visual processing in humans: a predictive coding framework. Neurosci Biobehav Rev 35:1237–1253

Rebai M, Bernard C, Lannou J, Jouen F (1998) Spatial frequency and right hemisphere: an electrophysiological investigation. Brain Cogn 36:21–29

Reich DS, Mechler F, Victor JD (2001) Temporal coding of contrast in primary visual cortex: when, what, and why. J Neurophysiol 85:1039–1050

Sceniak MP, Hawken MJ, Shapley R (2001) Visual spatial characterization of macaque V1 neurons. J Neurophysiol 85:1873–1887

Sclar G, Maunsell JH, Lennie P (1990) Coding of image contrast in central visual pathways of the macaque monkey. Vision Res 30:1–10

Sit YF, Chen Y, Geisler WS, Miikkulainen R, Seidemann E (2009) Complex dynamics of V1 population responses explained by a simple gain-control model. Neuron 64:943–956. doi:10.1016/j.neuron.2009.08.041

Stensaas SS, Eddington DK, Dobelle WH (1974) The topography and variability of the primary visual cortex in man. J Neurosurg 40:747–755

Vanegas MI, Blangero A, Kelly SP (2013) Exploiting individual primary visual cortex geometry to boost steady state visual evoked potentials. J Neural Eng 10:036003

Vanegas MI, Blangero A, Kelly SP (2015) Electrophysiological indices of surround suppression in humans. J Neurophysiol 113:1100–1109

Vassilev A, Manahilov V, Mitov D (1983) Spatial frequency and the pattern onset-offset response. Vision Res 23:1417–1422

Vassilev A, Mihaylova M, Bonnet C (2002) On the delay in processing high spatial frequency visual information: reaction time and VEP latency study of the effect of local intensity of stimulation. Vision Res 42:851–864

Wandell BA (1995) Foundations of vision. Sinauer Associates, Incorporated, Sunderland. doi:10.1002/col.5080210213

Wandell BA, Dumoulin SO, Brewer AA (2009) Visual cortex in humans. In: Encyclopedia of neuroscience, vol 10. Elsevier, Amsterdam, pp 251–257. doi:10.1016/B978-008045046-9.00241-2

Wang F et al (2016) Predicting perceptual learning from higher-order cortical processing. Neuroimage 124:682–692. doi:10.1016/j.neuroimage.2015.09.024

Widmann A, Schroger E (2012) Filter effects and filter artifacts in the analysis of electrophysiological data. Front Psychol 3:233 doi:10.3389/fpsyg.2012.00233

Zhang X, Zhaoping L, Zhou T, Fang F (2012) Neural activities in V1 create a bottom-up saliency map. Neuron 73:183–192

Zhang GL, Li H, Song Y, Yu C (2015) ERP C1 is top-down modulated by orientation perceptual learning. J Vis 15:8. doi:10.1167/15.10.8